JOURNAL OF MATERIALS SCIENCE 27 (1992) 2389–2396

Influence of cooling rates on the transformation behaviour of 9Cr–1Mo–0.07C steel

S. SAROJA, M. VIJAYALAKSHMI, V. S. RAGHUNATHAN
Physical Metallurgy Section, Metallurgy Division, Indira Gandhi Centre for Atomic Research, Kalpakkam 603 102, India

The choice of various decomposition mechanisms of austenite in a 9Cr–1Mo–0.07C steel under different rates of cooling has been studied. The techniques employed were electron probe micro-analysis, X-ray diffraction and electron microscopy. The observed morphological features may be explained based on the predominance of the two types of transformation, austenite → martensite and austenite → ferrite during cooling. In the steel used in this study, decomposition of austenite to proeutectoid ferrite was favoured at cooling rates less than about 2 Ks^{-1}. The mechanism by which the supersaturated proeutectoid ferrite relieves its excess solute concentration was also studied. A "microstructural map" has been proposed to predict the constitution at the end of any given cooling rate for 9Cr–1Mo–0.07C steel. The choice of commercial treatment has been rationalized with respect to the resultant microstructural constituents.

1. Introduction

Recent developments of high power, fast breeder reactor (FBR) technology have emphasized the need for developing materials with better void swelling and creep resistance as compared to the existing austenitic steels, for core component applications [1]. Of late, "ferritics" like 2.25Cr–1Mo, 9Cr–1Mo, 9Cr–2Mo, 10Cr–2Mo–V–Nb, 12Cr–2Mo, HT9, D57B, etc., are being considered for replacing the conventional "austenitics". These steels have a high resistance to void formation during ion, electron and neutron irradiations in the temperature range 673–898 K and this characteristic has rendered them suitable for application as fuel element components, such as wrappers, and also in the steam circuitry in the sodium-cooled fast reactors [1].

Of the various candidate materials, 9Cr–1Mo steels are being seriously considered for FBR applications for the following reasons [2–8]:

1. acceptable mechanical properties at service temperature, achieved by the fine substructure generated during martensitic transformations;
2. easy control of microstructure and microstructural stability during long-term service;
3. reduced tendency for temper embrittlement due to a lesser degree of segregation of impurity elements;
4. resistance to decarburization; and
5. better corrosion resistance.

These advantages have enabled the prototype fast reactor in the United Kingdom to use these steels as superheater components in steam generator circuits. They are also being considered for possible use as wrapper material. However, the main drawbacks of these steels appear to be their poor fabricability and high values of ductile to brittle transition temperatures.

The 9Cr–1Mo steels, in the normalized state, derive their strength basically from martensites which are formed during air cooling. The strength of martensite, α', arises from the presence of interstitial elements and a dislocation substructure [2–4]. 9Cr–1Mo steels in the normalized and tempered condition, depend on solid solution and precipitation strengthening of the matrix. The steel in this state has a high value of stress rupture ductility which remains constant even up to 50 000 h, as a consequence of its microstructure, which contains relatively coarse but evenly distributed carbides in the tempered martensite matrix. Although these steels have been studied in detail with respect to their microstructure and mechanical properties, most of these studies are confined to the commercially heat-treated and aged condition. It is considered that systematic development of a physical metallurgy data base with respect to various parameters such as cooling rate, austenitizing temperature, tempering treatment, carbon content, etc., is necessary. This paper presents the first part of our results of an experimental programme aimed at developing the required data base on a 9Cr–1Mo steel.

The various types of transformation that take place in a 9Cr–1Mo–0.07C steel after austenitizing at 1323 K for 30 min and cooled at various rates, are discussed. The decomposition of austenite, γ, is found to proceed through different mechanisms depending on the rate of cooling, which in turn introduces considerable differences in the resultant constitution. The

0022–2461

transformation scenario at different temperature regimes to which the steel is exposed during cooling is clearly demonstrated in this paper, based on which a "microstructural map" for 9Cr–1Mo–0.07C steel under different cooling rates has been proposed. The choice of the conditions for the commercial heat treatment of this steel has also been rationalized in this study. The resultant microstructure and its influence in improving the properties of the 9Cr–1Mo steel have been discussed.

2. Experimental procedure

The composition of the steel used in this study is listed in Table I. Specimens of dimensions 12 mm × 12 mm × 12 mm were solution annealed at 1323 K for 30 min and cooled by different techniques: (i) water quenching (100 Ks^{-1}), (ii) oil quenching (20 Ks^{-1}), (iii) air cooling (2 Ks^{-1}), (iv) furnace cooling (0.1 Ks^{-1}), and (v) air cooling followed by a tempering treatment at 1023 K for 60 min (the commercial treatment). The first two fast cooling rates, Q_f^1 and Q_f^2, were calculated based on available information on relative cooling rates in different quenching media [2]. The latter two slow cooling rates, namely air cooling and furnace cooling, Q_s^1 and Q_s^2, were measured.

The heat-treated samples were polished and etched with Vilella's reagent followed by gold coating for metallographic observations. Measurements of prior austenite grain size, area fraction of ferrite, α, packet size of martensite, etc., were made using a Philips scanning electron microscope (Model PSEM501). Vickers macro- and micro-hardness measurements were carried out on various regions of the sample using a load of 1 kg and 100 g, respectively. For the air-cooled and furnace-cooled samples, micro-hardness measurements were also made with lower applied loads in order to establish the variation in hardness between the two microstructural constituents.

Chemical analysis of iron, chromium, molybdenum, manganese and carbon in the martensite and ferrite regions was carried out using a Cameca SX-50 electron probe micro analyser (EPMA), in order to obtain the redistribution of solute elements. A large number of points comprising both ferrite and martensite spanned over a region of 150 μm was chosen for the analysis and measurements were made at appropriate intervals. The EPMA operating conditions were maintained constant during the analysis at the following values: acceleration voltage 20 kV, regulated beam current 20 nA, X-ray take off angle 40°, beam diameter ≃ 1 μm and a counting time of 10 s. The K_α radiation of iron, chromium and manganese were diffracted by an LiF crystal, that of carbon by a PC1 crystal and the L_α radiation of molybdenum by a PET crystal. The X-ray intensities of the above radiations were also measured on standards (pure iron, chromium, molybdenum, manganese and diamond) under identical conditions of analysis. The composition values were obtained after correction for the atomic number, absorption and fluorescence effects (ZAF correction).

TABLE I Composition of the steel used in the present study

Element	Composition (wt %)
Cr	8.24
Mo	0.955
Mn	0.356
C	0.072
P	0.0206
Si	0.265
Fe	Balance

3. Results and discussion

The austenitizing treatment was carried out at 1323 K for 30 min, in the present study. It is well known that Cr–Mo steels of this type could exist in any one of the various phase fields, such as α + γ, γ, γ + δ-ferrite, depending on the composition of the alloy and austenitizing temperature employed. The choice of austenitizing temperature (1323 K) for the alloy used has been arrived at based on the fact that this temperature lies well within the austenite phase field, when the net chromium equivalent of this alloy is estimated by an expression of the type:

$$\text{net chromium equivalent} = \%Cr + 6\,(\%Si) + 4\,(\%Mo) - 40\,(\%C) - 2\,(\%Mn) \quad (1)$$

and superimposed on the equilibrium diagram of the Fe–Cr system [9]. Another reason for the choice of 1323 K as the austenitizing temperature is based on the expectation that the pre-existing carbide particles, if any, would completely go into solution at this temperature. However, for temperatures lower than 1300 K it has been reported [10] that there was a partial retention of $M_{23}C_6$ carbides which were intentionally precipitated prior to austenitizing treatment. It has been proposed that there is preferential nucleation of austenite along the ferrite/carbide interface, wherein the carbide particles are enveloped by austenite and subsequent growth depends on diffusion of carbon through austenite as carbides dissolve [2]. In the present work, the steel used was in the normalized and tempered condition, wherein $M_{23}C_6$ is expected to be present. In addition, the use of an unstabilized variety of steel and higher austenitizing

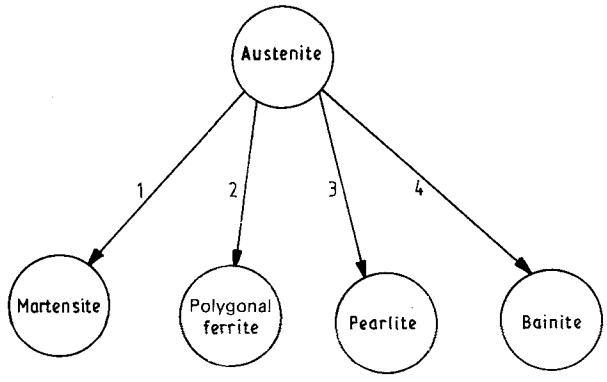

Figure 1 Possible decomposition mechanisms of austenite.

temperature ensure complete dissolution of all pre-existing carbides during the austenitizing treatment.

It is well established that austenite in steels could undergo either one or a combination of decomposition processes, while it is cooled to room temperature, as shown in Fig. 1. The transformation path favoured by the alloy and the resultant constitution at the end of cooling, depends largely on the initial alloy content and the rate of cooling. In the present study of 9Cr–1Mo steel, the decomposition of austenite proceeds through either the transformation path 1 or a combination of paths 1 and 2 depending on the cooling rates employed, as can be seen below.

3.1 Decomposition mechanisms of austenite

Fig. 2a–d show scanning electron micrographs of the steel cooled to room temperature at various rates of cooling. The uniformity of microstructures across various sections of the specimen and the small dimensions of the specimens used suggest that the rate of cooling was constant within the sample. It is seen that there is considerable variation in the morphology and nature of the microstructural constituents with cooling rate. The two rapid cooling rates (Q_f^1 and Q_f^2), employed in the present study resulted in the complete transformation of austenite to martensite, α' (Fig. 2a and b). In contrast, the slower cooling rates (Q_s^1 and Q_s^2) favoured the formation of proeutectoid ferrite and martensite (Fig. 2c and d). The *CCT* diagrams developed for 9Cr–1Mo steel, based on Jominy hardenability tests, show [9] that there is a range of cooling rates over which complete transformation of austenite to martensite is expected. However, cooling rates slower than a certain critical value, Q_c, would promote the formation of proeutectoid ferrite, the value of which depends on the net chromium equivalent. In the present study, where the net chromium equivalent of the steel is 10.2, it is seen that Q_f^1 and Q_f^2 are higher than Q_c, thereby suppressing the formation of proeutectoid ferrite, while Q_s^1 and Q_s^2, being lower than Q_c, result in the growth of ferrite. The complete transformation of austenite to martensite preferentially at rapid cooling rates can be understood in terms of non-availability of sufficient time in the high-temperature transformation range to effect nucleation and growth of proeutectoid ferrite. Detailed microscopic investigations have shown that the basic units of martensites in Figs. 2a and b are the "lath type", that are aligned parallel to one another in groups, or "packets". The present observation of lath-type martensite is consistent with the high value of M_s temperature (673 K) reported for this steel. It is expected that the morphology of martensite will be controlled by the yield strength of austenite. Therefore, the lath-type martensite, which is basically accommodated by slip (a high-temperature deformation process) is normally associated with high M_s values.

A comparison of Fig. 2c and d, would clearly reveal that the proeutectoid ferrite grains which are present after slower cooling, Q_s^1 and Q_s^2 have regular-shaped boundaries; they are not acicular but equiaxed polygonal ferrite. The width of the ferrite grain as well as

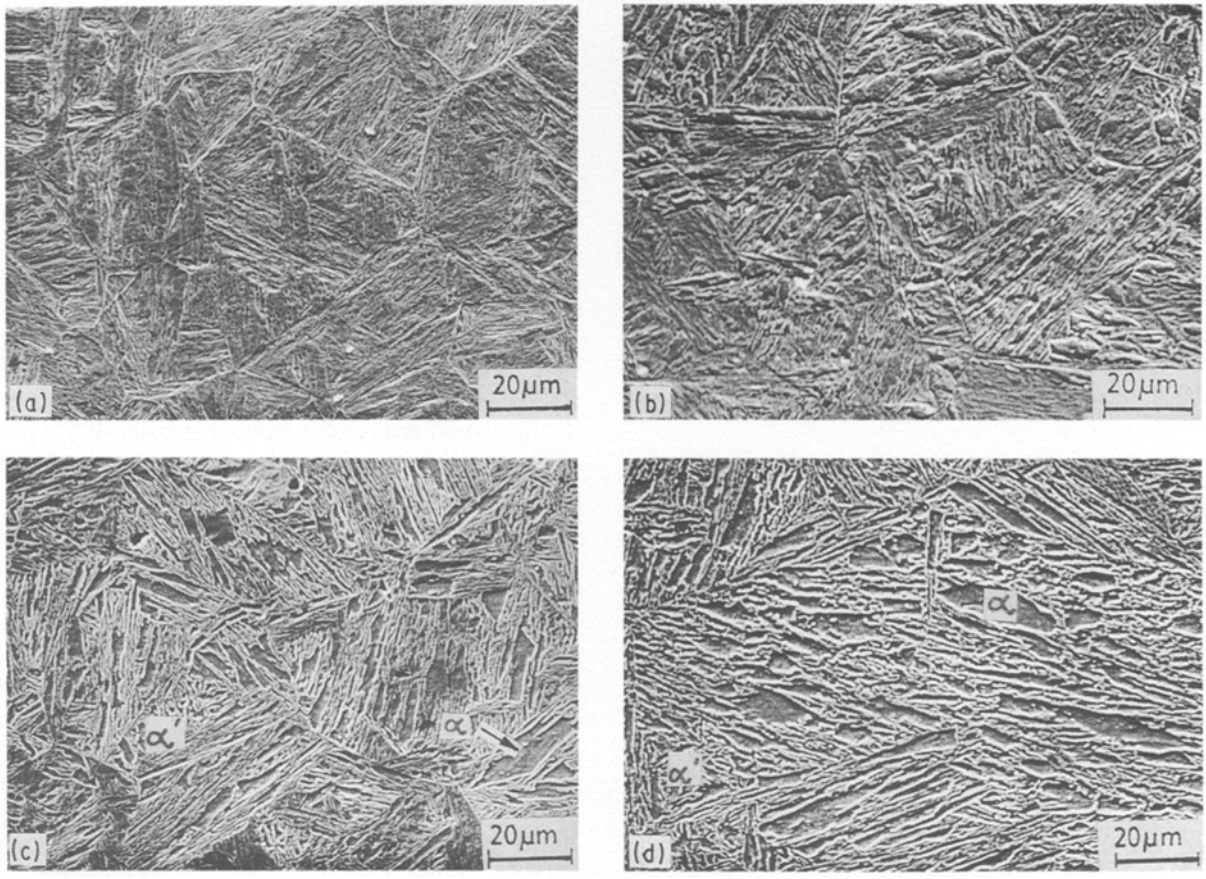

Figure 2 Scanning electron micrographs of 9Cr–1Mo–0.07C specimens austenitized at 1323 K for 30 min and cooled at different rates: (a) 100 Ks^{-1}, (b) 20 Ks^{-1}, (c) 2 K s^{-1}, (d) 0.1 Ks^{-1}.

the amount of ferrite increases with decreasing cooling rate. The morphology of the proeutectoid ferrite shown in Fig. 2c and d clearly confirms that the ferrite has grown by a conventional nucleation and growth mechanism and not by either massive transformation of austenite or as Widmanstätten plates. Based on Fig. 2c and d, it is reasonable to expect that in slowly cooled steels, part of the austenite has transformed to ferrite in the high-temperature range 873–1073 K, leaving the remaining austenite to undergo martensitic transformation as the steel is exposed to temperatures below 673 K (which is the M_s temperature reported for this steel), before it is cooled to room temperature.

The uniform dispersion of fine proeutectoid ferrite in a martensitic matrix during air cooling of the present alloy (Fig. 2c) is not expected, in view of the fact that the experimentally determined cooling curve during air cooling does not intersect the available *TTT* diagram [10]. Moreover, the formation of ferrite has not been cited in any of the earlier studies [11], based on which air cooling has been chosen for even commercial treatment. Therefore, more detailed microscopic studies were carried out to unambiguously confirm the presence of ferrite in air-cooled samples. Fig. 3 shows the conclusive evidence for the formation of proeutectoid ferrite during air cooling. In addition, the presence of proeutectoid ferrite is expected considerably to reduce the microhardness value within ferrite, compared to the adjacent martensitic matrix. An attempt to monitor the variation of microhardness value (using a conventional applied load of 100 g) between the two microstructural constituents, α and α', in air-cooled samples was not successful, probably due to the fine size of the ferrite grains. Therefore, microhardness values were measured with a lower applied load of 15 g. It is realized that the use of such small loads would reduce the reliability of the measurements, due to the load dependence of microhardness. However, for the restricted purpose of evaluating the relative difference in the microhardness between α and α', the choice of small load was considered justified. It is observed that the microhardness value of the ferrite grains is about 355 VHN (load = 15 g), which is significantly lower than that of the adjacent α' matrix 568 VHN (for the same load). Thus, it can be confirmed beyond doubt that the proeutectoid ferrite forms during air cooling of the steel. The present observation of ferrite in contrast to its absence in earlier studies, can only be rationalized based on the difference in the carbon content of the different steels used.

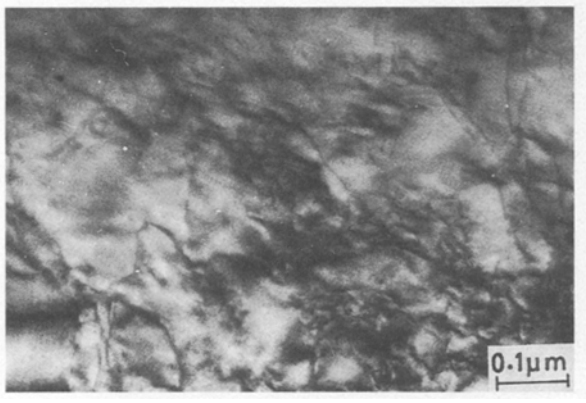

Figure 3 Evidence for the formation of proeutectoid ferrite in a 9Cr–1Mo–0.07C steel austenitized at 1323 K and air cooled.

It has been well established that the grain boundaries of austenite are the preferred sites for the nucleation of proeutectoid phases and that the grain size of the parent austenite phase is directly related to the size of the transformation products. The parameters chosen for the complete microstructural description of the steel are as follows: prior austenite grain size, constitution, area fraction of proeutectoid ferrite, packet size of martensite, macro- and micro-hardness. Based on a large number of observations, the variations in the values of these parameters with different cooling rates are listed in Table II. It is seen that the size of prior austenite grains is about 45 μm which is comparable to the values reported in the literature for similar austenitizing treatment [10]. The microstructural constituents at the end of various cooling rates are found to change from 100 % martensite in rapidly cooled steel to a mixture of proeutectoid ferrite and martensite in slowly cooled samples. The observed change in the constitution could be attributed to the difference in the transformation paths of austenite during various cooling rates. The size and area fraction of proeutectoid ferrite in furnace-cooled samples are much larger than those in air-cooled samples, as a result of longer "stay time" in the high-temperature transformation region.

From Table II, it is seen that the packet size remains constant for the fast cooling rates employed, where there is complete transformation to martensite. The measurement of packet size in slowly cooled samples was found to be quite difficult owing to the lack of clarity in defining the boundary of each packet. However, the average value of packet size for Q_s^1 and Q_s^2 is much lower than those corresponding to Q_f^1 and Q_f^2. The range of packet size has also increased suggesting that there is a large variation in the packet size from one region to another. The observed decrease in the packet size with slower cooling rates could have been caused by the presence of proeutectoid ferrite formed prior to martensite during slow cooling. The ferrite grains would reduce the number density of γ/γ interfaces which are the nucleation sites for the martensite laths. Moreover, the growth of martensite laths would artificially be terminated at the ferrite/austenite interface due to the existence of ferrite. It is reasonable to expect that the advancing interface between the martensite and the untransformed austenite would have grown until its impingement at the adjacent austenite grain boundary, if only the ferrite was not present. Thus the observed reduction in the packet size for slower cooling rates is not considered a genuine effect of rate of cooling on packet size, but rather a consequence of the transformation of austenite to ferrite in the higher temperature range during cooling. It has been reported that the packet size, which is a key factor in determining the strength of martensitic steels, is controlled mainly by the change

TABLE II Prior austenite grain size and effect of cooling rate on constitution, amount of ferrite, martensite packet size, macro- and micro-hardness values

Treatment	Cooling rate	Prior austenite grain size	Constitution	Amount of ferrite	Martensite packet size	Hardness, load = 1 kg	Micro-hardness, Load = 100 g	
							Ferrite (VHN)	Martensite (VHN)
	(Ks^{-1})	(μm)		(%)	(μm)	(VHN)		
Q_f^1	100	40–45	α′	0	12–14	400	–	403
Q_f^2	20	40–45	α′	0	12–14	377	–	397
Q_s^1	2	40–45	α + α′	< 4	6–10	399	355[a]	568[a]
Q_s^2	0.1	40–45	α + α′	10–12	4–10	398	230[b]	439[b]

[a] Load = 15 g.
[b] Load = 50 g.

in the prior austenite grain size [2]. The constancy in the observed values of packet size with the cooling rates is reflected in the constancy of the hardness values. However, a decrease in the packet size, if caused by lowering the austenitizing temperature, has been reported to increase hardness levels [10]. More accurate measurements of yield strength values have even suggested that the variation of yield strength with packet size obeys the Hall–Petch relation [2].

3.2 Transformations in proeutectoid ferrite

In addition to the changes in the decomposition processes of austenite during various cooling rates, another interesting feature is the mechanism by which the high supersaturation of carbon within the proeutectoid ferrite is expected to be relieved. It is well known that the equilibrium solubility in proeutectoid ferrite at the eutectoid temperature, 1000 K, is 0.02 wt %C, much lower than the initial carbon content of the alloy studied. Such a carbon supersaturation in ferrite can be relieved either by precipitation within ferrite or by partitioning of carbon into the residual austenite, both of which could proceed quite rapidly. Repartitioning of carbon between ferrite and residual austenite (or martensite) has been cited [12, 13] using various techniques, such as atom probe analysis, analytical electron microscopy and EPMA. However, most of these studies reporting solute redistribution during cooling have used an atom probe analyser. Studies where more reliable quantitative results using EPMA are reported, have resorted to tempering treatments subsequent to cooling. In the present study, electron probe microanalyses of all the elements were carried out in order to identify the process through which supersaturation of ferrite, formed at high temperature, is relieved. Although it is generally expected that there would not be rearrangement of substitutional atoms such as chromium, molybdenum and manganese, the exact composition of all the elements was measured across a ferrite–martensite–ferrite region. Among the various thermal treatments employed in the present study, the difference in the post-transformation composition of carbon between ferrite and martensite is likely to be a maximum after tempering at 1023 K. However, no confirmation of a significant redistribution of carbon or any other element, could be obtained on the tempered sample, as is seen in Fig. 4. This figure also includes the identity of the microstructural constituents across which the compositions were evaluated using EPMA. These results clearly confirm the absence of any partitioning of substitutional atoms such as manganese, chromium and molybdenum during the transformation. It is expected that the post-transformation composition need not correspond to that existing during the two transformations, namely

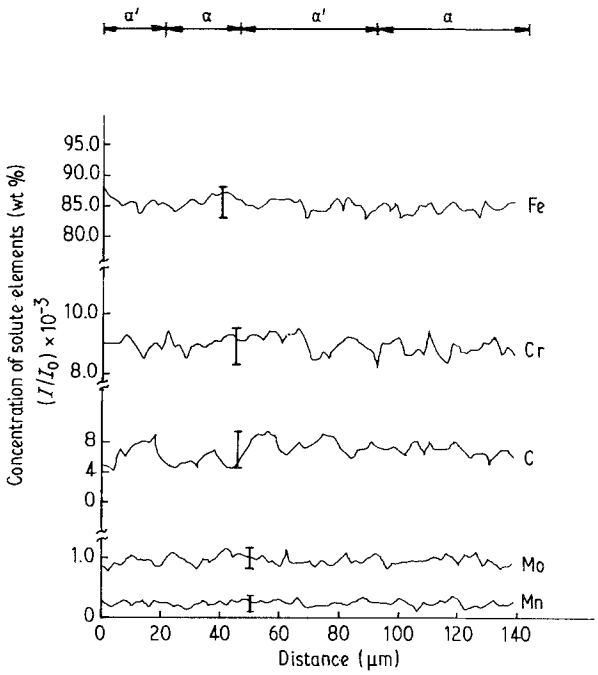

Figure 4 Electron probe micro analyses of iron, chromium, manganese, molybdenum and carbon in a 9Cr–1Mo–0.07C sample normalized at 1323 K for 30 min, followed by tempering at 1023 K for 60 min and air cooling. The amount of carbon has been expressed as normalized intensity ratio, because it was aimed to determine only the relative variations in the carbon content across various regions.

$$\gamma \rightarrow \alpha \text{ (1073–873 K)}$$

and

$$\gamma \rightarrow \alpha' \text{ (} < 690 \text{ K)}$$

However, it would give an idea as to whether any repartitioning of solute elements had occurred during the high-temperature transformation. If any redistribution of interstitial atoms had occurred during the high-temperature transformation, the remaining austenite during transformation into martensite at 673 K

would inherit the carbon content of the austenite at the end of the $\gamma \rightarrow \alpha$ transformation. The present results show that there have been no such rearrangements, at least within the statistical error in measurements of solute concentration using EPMA. However, earlier investigations on plain low-carbon steels have shown that the carbon content in ferrite, as determined by EPMA, is 5–10 times lower than that of martensite regions [14].

Apart from a simple redistribution of carbon between ferrite and austenite, another way of relieving supersaturation of carbon in the ferrite is by precipitation of carbides, which could proceed by any one of the following mechanisms.

1. "Interphase precipitation", wherein the removal of carbon trapped at the interface is a prerequisite for further advancement of γ/α interface. Such a sequence of events (Fig. 5) would lead to the precipitation of "fibrous carbides", as in vanadium steels [15, 16].
2. Precipitation of Fe_3C at the γ/α interface which subsequently (< 673 K) would have transformed to the α'/α interface [17].
3. Nucleation and growth of carbides within the ferrite grains, subsequent to its formation.

Fig. 6 shows the microstructure of martensite and ferrite regions in a furnace-cooled sample Q_s^2. It is seen that there is no evidence for precipitation of either "fibrous carbides" or Fe_3C at the α'/α interface. However, uniform dispersion of fine needle-like carbides is seen in the ferrite region. These precipitates are found to be rich in iron and hence expected to be M_3C. This observation confirms that the supersaturation of carbon in proeutectoid ferrite is, indeed, relieved by precipitation of carbides within α, subsequent to the formation of α grains from γ and not by repartitioning of carbon across the γ/α interface. Based on the present studies, the sequence of transformation of austenite in 9Cr–1Mo–0.07C steel during various cooling rates can be summarized as follows:

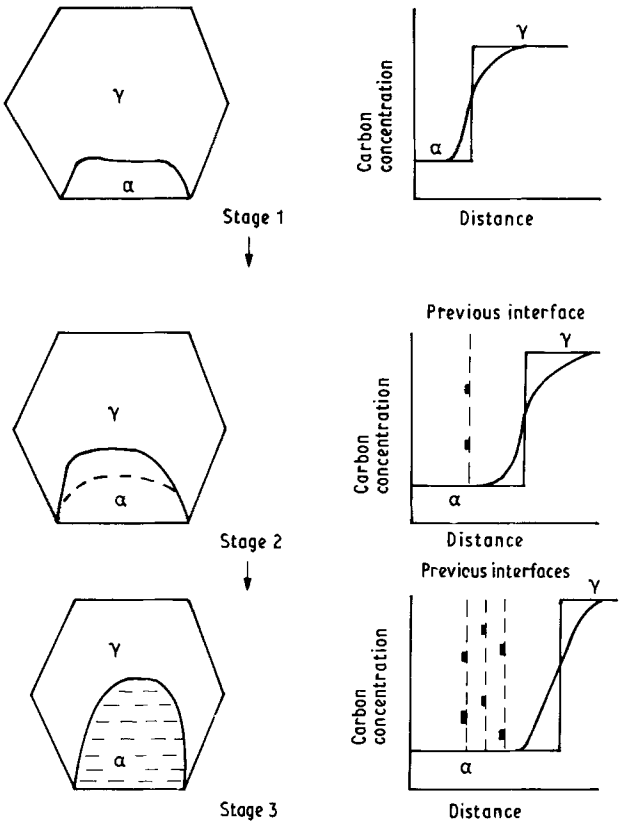

Figure 5 Schematic representation of a sequence of events in an interphase precipitation (γ/α interface), accompanying the transformation of austenite to ferrite during cooling. The expected repartitioning of carbon between γ and α is shown adjacent to each stage.

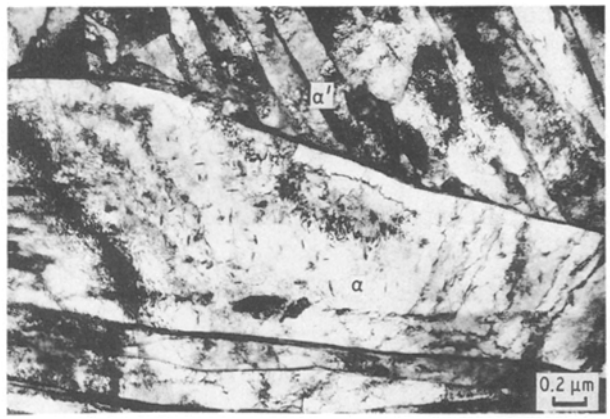

Figure 6 Micrograph of 9Cr–1Mo–0.07C steel austenitized at 1323 K for 30 min and furnace cooled. Needle-like precipitates of M_3C within ferrite grains are seen. No precipitates are observed along the α'/α interface.

$$\gamma \xrightarrow{Q_f^1} \alpha'$$
$$\gamma \xrightarrow{Q_f^2} \gamma + \text{super saturated } \alpha \rightarrow \gamma_{residual} + (\alpha + M_3C)$$
$$\gamma \xrightarrow{Q_s^1} \gamma + \text{super saturated } \alpha \rightarrow \gamma_{residual} + (\alpha + M_3C)$$
$$\rightarrow \alpha' + \alpha + M_3C$$

The microstructural map generated for this steel under various cooling rates is superimposed on an isothermal *TTT* diagram developed by Pickering and Vassiliov [10], for an austenitizing temperature of 1273 K. The time–temperature data obtained during cooling in the present study are also shown in the diagram, Fig. 7. In the present study, although the austenitizing temperature is 1323 K, superimposition of these data on a *TTT* diagram obtained at 1273 K is considered valid as it is reported [10] that the shift in the *TTT* diagram between 1273 and 1373 K is not significant. The expected microstructures in the four different transformation regimes for the slowest cooled steel, Q_s^2, are also predicted in Fig.7.

3.3. Microstructural rationalization of commercial heat treatment

The commercial heat treatment adopted for the 9Cr–1Mo variety of steels with 0.1 % C, consists of austenitizing at 1323 K for 30 min, air cooling followed by tempering at 1023 K for 60 min for small thickness. The microstructural basis for this particular choice of heat treatment is very well brought out by the present studies, though these pertain to 0.07 % C.

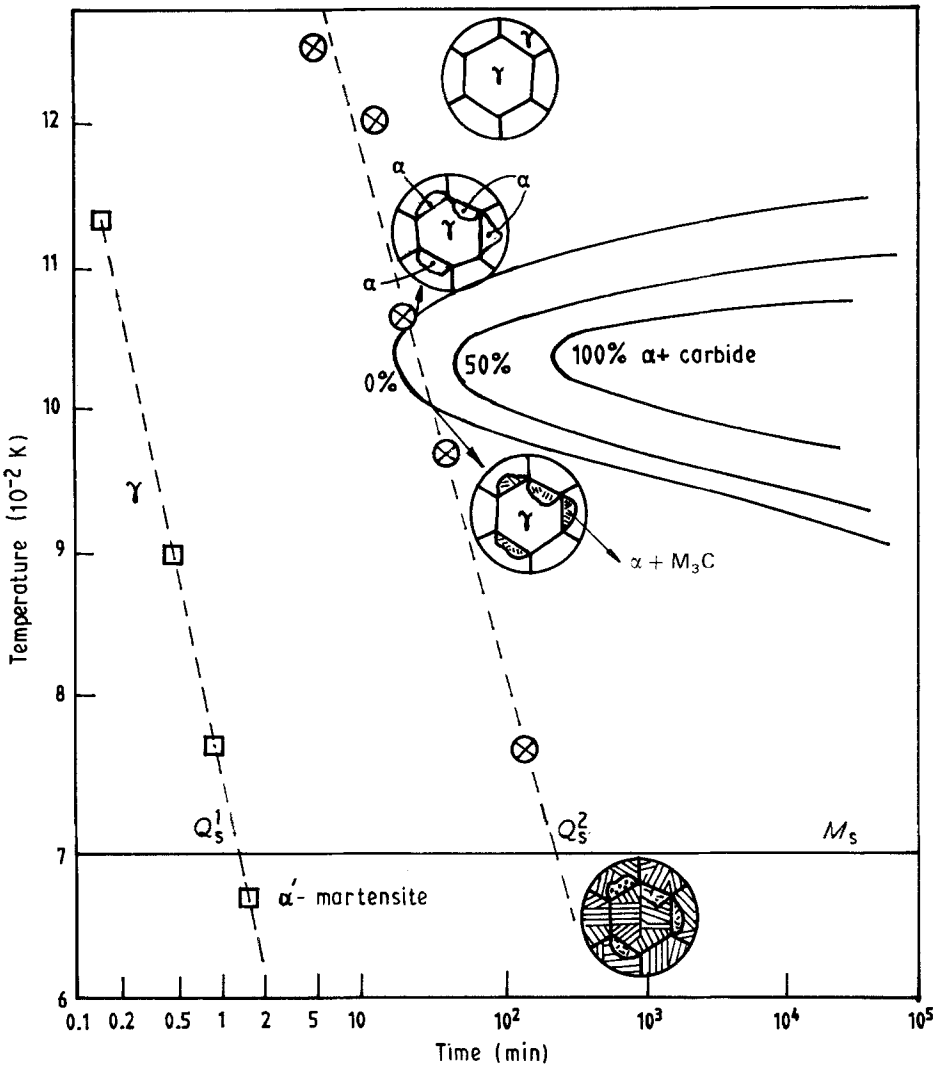

Figure 7 Microstructural map of a 9Cr–1Mo–0.07C steel austenitized at 1323 K for 30min and furnace cooled, superimposed on a *TTT* diagram [10]. The experimental points of time and temperature obtained during (⊡) air cooling and (⊗) furnace cooling of the specimens are also shown.

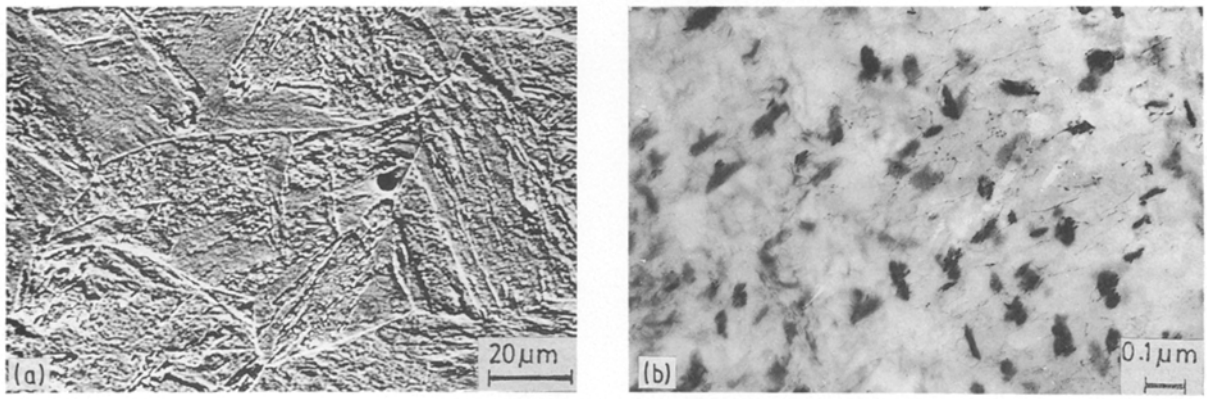

Figure 8 (a) Micrograph of a 9Cr–1Mo–0.07C steel austenitized at 1323 K for 30 min, air cooled and tempered at 1023 K for 60 min and air cooled. (b) Direct evidence for the precipitation of M_3C needles in ferrite in commercially heat-treated steel.

Fig. 8a shows a scanning electron micrograph of the steel which has received the above commercial treatment. It is seen that there is considerable reversion of martensite during tempering treatment. Detailed microscopic studies have shown that there are fine needle-shaped M_3C carbides in ferrite regions, as can be seen from the micrograph in Fig. 8b. It is found that the tempering treatment promotes the following transformations: (i) reversion and tempering of martensite, and (ii) precipitation and strengthening of soft ferrite by uniform dispersion of fine M_3C. These reactions have resulted in a considerable decrease in the average hardness level up to 230 VHN. A large number of microhardness measurements have confirmed that there is no significant change in microhardness from one region to another. Thus, the commercial treatment has rendered a steel with adjacent regions which are strengthwise compatible with each other.

The specific choice of conditions of heat treatment for commercial purposes is based on extensive structure–property correlation studies on 9Cr–1Mo steels. These studies have confirmed that this treatment (1323 K/min/air cooling followed by 1023 K/60 min/air cooling) for small-sized specimens produces the steel with the best combination of high-temperature properties.

The uniform dispersion of M_3C carbides shown in Fig. 8b during commercial heat treatment, is expected to impart an even distribution of strain accumulation, between matrix and grain-boundary regions, under creep conditions, leading to (i) the absence of grain-boundary cavitation after creep testing of tempered 9Cr–1Mo steels, and (ii) acceptable values of creep and rupture strength which are independent of grain size. Based on microstructural studies after long-term exposures at high temperature, the tempered martensite microstructure (shown in Figs. 8a and b) has been reported to be very stable and this is mainly responsible for the observed minimum exhaustion of creep ductility during their long-term use in service (50 000h). The M_3C particles not only hinder the movement of dislocations but also retard the recovery of the structure, thus retaining the creep resistance. The optimum microstructure is achieved when the inter-carbide spacing and size are small [18]. Hence, the choice of conditions of commercial heat treatment to yield a resultant microstructure with a uniform dispersion of M_3C carbides can be rationalized based on the above reasons.

4. Conclusions

Decomposition mechanisms of austenite in 9Cr–1Mo–0.07C steel at various cooling rates have been studied.

1. The austenite decomposes completely to martensite at high cooling rates (100–20 Ks^{-1}), in contrast to a mixture of martensite and proeutectoid ferrite at slower cooling rates (2–0.1 Ks^{-1}).

2. The proeutectoid ferrite does not reject its excess carbon into the γ/α interface, as is normally expected in many steels. However, the supersaturation is relieved by precipitation of M_3C within the ferrite, subsequent to its formation.

3. A "microstructural map" is proposed to predict the type of transformation the austenite would undergo at various cooling rates, in 9Cr–1Mo–0.07C steel.

4. The choice of heat-treatment conditions for the commercial application of 9Cr–1Mo steel, has been rationalized, based on microstructural observations and their impact on the relevant properties.

Acknowledgements

The authors thank Dr Placid Rodriguez, Head, Metallurgy and Materials Programme, and Mr J. B. Gnanamoorthy, Head, Metallurgy Division, for their keen interest and constant encouragement during the course of this work.

References

1. E. A. LITTLE, in "Proceedings of the International Conference on Materials for Nuclear Reactor Core Applications", Vol. 2, Bristol, October 1987 (British Nuclear Energy Society, London 1988) p. 47.
2. G. KRAUSS, in "Principles of heat treatment of steels" (American Society for Metals, Metals Park OH, 1980) pp. 43, 127, 161.
3. T. E. SWARR and G. KRAUSS, *Met. Trans.* **7A** (1976) 41.
4. T. E. SWARR and G. KRAUSS, in "Grain Boundaries in Engineering Materials", edited by J. L. Walter, J. H. Westbroof and D. A. Woodford. (Claitor's, Baton Rouge, LA, 1975) p. 127.
5. G. R. SPEICH and W. C. LESLIE, *Met. Trans.* **3** (1972) 1043.
6. O. N. CARLSON and H. INDIRAWIRAN, in "Proceedings of a Topical Conference on Ferritic alloys for use in Nuclear Energy Technologies", Snowbird, UT, June 1983, edited by J. W. Davis and D. J. Michel (The Metallurgical Society of AIME, New York, 1984) p. 559.
7. W. L. BELL, T. LAURITZEN and S. VAIDYANATHAN, *ibid.*, p. 113.
8. C. WILLBY and J. WALTERS, in "Proceedings of an International Conference on Ferritic Steels for Fast Reactor Steam Generators", London, June 1977, edited by S. F. Pugh and E. A. Little (British Nuclear Energy Society, London, 1978) p. 40.
9. S. J. SANDERSON, in "Proceedings of an ASM International Conference on Production, Fabrication, Properties and Applications of Ferritic Steels for High Temperature Applications", Warren, PA 1981, edited by Ashok K. Khare (ASM, Metals Park OH, 1982) p. 85.
10. F. B. PICKERING and A. D. VASSILIOV, *Metals Tech.* (1980) 409.
11. J. ORR, F. R. BECKITT and G. D. FAWKES, in "Proceedings of an International Conference on Ferritic Steels for Fast Reactor Steam Generators", London, June 1977, edited by S. F. Pugh and E. A. Little (British Nuclear Energy Society, London, 1978) p. 91.
12. H. K. D. H. BHADESHIA and A. R. WAUGH, *Acta Metall.* **30** (1982) 775.
13. A. D. ROMIG and J. I. GOLDSTEIN, *Met. Trans.* **11A** (1980) 1151.
14. V. BISS and R. L. CRYDERMAN, *ibid.*, **2** (1971) 2267.
15. R. W. K. HONEYCOMBE, *ibid.*, **7A** (1976) 915.
16. R. W. K. HONEYCOMBE and F. B. PICKERING, *ibid.*, **3** (1972) 1099.
17. S. J. SANDERSON, in "Proceedings of an International Conference on Ferritic Steels for Fast Reactor Steam Generators", London, June 1977, edited by S. F. Pugh and E. A. Little (British Nuclear Energy Society, London, 1978) p. 120.
18. J. WOODHEAD and A. G. QUARRELL, *JISI* **203** (1965) 605.

Received 7 January
and accepted 7 June 1991